Smart Outriggers for Seismic Protection of High-rise Buildings

Chia-Ming Chang & Takehiko Asai
University of Illinois at Urbana-Champaign, USA

Zhihao Wang
North China Institute of Water Conservancy and Hydroelectric Power, China

Billie F. Spencer, Jr.
University of Illinois at Urbana-Champaign, USA

Zhengqing Chen
Hunan University, China

SUMMARY:
High-rise buildings are a common feature of urban cities around the world. These flexible structures frequently exhibit large vibration due to strong winds and earthquakes. Structural control has been employed as an effective means to mitigate excessive responses; however, structural control mechanisms that can be used in tall buildings are limited primarily to mass and liquid dampers. An attractive alternative can be found in outrigger damping systems, where the bending deformation of the building is transformed into shear deformation across dampers placed between the outrigger and the perimeter columns. The outrigger system provides additional damping that can reduce structural responses, such as the displacements and floor accelerations. This paper first investigates the potential of using smart dampers, specifically magnetorheological (MR) fluid dampers, in the outrigger system. The efficient and feasible configuration of the outrigger damping system in terms of damper size and location also is considered. With the technique of real-time hybrid simulation approach, the developed smart outrigger system is experimentally examined and verified through a small-scale setup. In this test, a MR damper performs resisting force against earthquake loadings that is generated from a servo-hydraulic actuator, and the structural system is concurrently simulated in a computer. As a result from the experiment, the smart outrigger system demonstrates the efficacy for mitigating structural responses through semi-active control under seismic excitations.

Keywords: Smart Outrigger, Seismic Control, Real-time Hybrid Simulation

1. INTRODUCTION

Buildings have continued to soar skyward with the development of new materials and construction technologies. However, such flexible structures may fall victim to excessive levels of vibration caused by strong winds and earthquakes. As a result, structural modifications ranging from alternative structural systems and aerodynamic changes to utilization of passive and active control devices have been suggested for protecting flexible structures against external disturbances (Kareem et al. 1999).

To protect high-rise buildings from excitations induced by natural hazards, an innovative approach is the outrigger damping system, consisting of vertical dampers between outrigger walls and perimeter columns in a frame-core tube structure (Jeremlah 2006). A conventional outrigger cantilevers from the core to the perimeter columns, resulting in the resisting moment against static lateral loads (Smith and Salim 1981). Jeremlan (2006) and Smith and Willford (2007) proposed adding dampers to the outrigger to enhance structural dynamic performance against wind loadings. Willford et al. (2008) also report implementation this technique in a high-rise building in the Philippines.

Magnetorheological (MR) dampers have been experimentally verified to provide superior performance by an effective means of semi-active control strategies (Spencer et al. 1997). In an outrigger damping system, employing MR dampers may better mitigate structural responses; however, this approach is

yet to be proven. One of structural testing methods for rate-dependent devices is real-time hybrid simulation, which enables the capability of testing the physical damper experimentally and simulating the high-rise building numerically at the same time. By combining physical dampers with a numerical model, a complexly structural system can be explored in a laboratory without scaling structures, especially for high-rise building. Consequently, the performance using MR dampers can be also validated prior to installing them in a structure.

In this study, a smart outrigger damping system employing magnetorheological (MR) dampers is proposed for protecting tall buildings against the strong winds and seismic excitations. First, two type of simplified numerical models are developed with or without perimeter columns incorporated. An optimal damping coefficient in the damped outrigger is determined through the proposed evaluation criteria that will be used as a baseline for comparison. Semi-active control design facilitates a reduce-order model to generate controllers, and a clipped-optimal/LQG control algorithm (Dyke, et al. 1996) derives the controller for the MR dampers in the outrigger system. Numerical simulation of the semi-active controlled outrigger system is performed under two different ground motions. Moreover, the smart outrigger is implemented and experimental verified through real-time hybrid simulation in the case of the building model without considering perimeter columns. As a result, the proposed smart outrigger exhibits advanced capability of mitigating seismic responses in comparison to the viscously damped outrigger.

2. PROBLEM FORMULATION

A high-rise building can be idealized as a cantilevered beam in which the structural deformations are derived from the behavior of the core. Such an approach was employed to model a 76-story building in the ASCE benchmark control problem for the wind excited high-rise buildings (Yang et al. 2004). For a high-building with damped outriggers, the control devices (e.g., viscous dampers or MR dampers) are located between the outrigger walls and the perimeter columns. According to the model provided in Smith and Willford (2007), the perimeter columns are assumed to be axially very stiff, while the outrigger behaves as a rigid body. Nevertheless, neglecting the dynamics due to perimeter columns may overestimate performance of the damped outrigger system. Thus, high-rise buildings with damped outriggers should include the vertical motion of the perimeter columns in analysis, as shown in Figure 1. The numerical model of the structural system can be subsequently established by three components: a center core, the perimeter columns, and dampers. With an appropriate discretization, the equation of motion of the control problem can be written as

$$\begin{cases} \mathbf{M}\ddot{\mathbf{u}} + \mathbf{C}\dot{\mathbf{u}} + \mathbf{K}\mathbf{u} = \mathbf{\Lambda}(nef) - \mathbf{M}\mathbf{\Gamma}\ddot{x}_{\mathrm{g}} \\ \mathbf{M}_{\mathrm{c}}\ddot{\mathbf{u}}_{\mathrm{c}} + \mathbf{C}_{\mathrm{c}}\dot{\mathbf{u}}_{\mathrm{c}} + \mathbf{K}_{\mathrm{c}}\mathbf{u}_{\mathrm{c}} = \mathbf{\Lambda}_{\mathrm{c}}(nf) \end{cases} \tag{1}$$

where f is the force from a single control device; n is the total number of control devices; e is the distance of the control devices to the center of the core (see Figure 1); f_{m} is the total moments; $\mathbf{M}$, $\mathbf{C}$, $\mathbf{K}$ are the structural mass, damping, stiffness matrices of the center core; $\mathbf{M}_{\mathrm{c}}$, $\mathbf{C}_{\mathrm{c}}$, $\mathbf{K}_{\mathrm{c}}$ are the structural mass, damping, stiffness matrices for the perimeter columns; $\mathbf{u}$ is the structural deformation vector considering the bending behavior; $\mathbf{u}_{\mathrm{c}}$ is the axial deformation of the perimeter columns; $\mathbf{\Lambda}$ presents the location of the outrigger system with respect to a specific rotational degree of freedom (DOF); $\mathbf{\Lambda}_{\mathrm{c}}$ indicates the connection of the outrigger system at the perimeter columns; $\mathbf{\Gamma}$ is a vector whose element with respect to the translational DOFs are all unity and zero for others; $\ddot{x}_{\mathrm{g}}$ is the ground acceleration.

In control applications, the state-space representation is usually employed to form a structural system and subsequently to develop control strategies. The overall structural system is converted from Eq. (1) and represented as

$$\begin{aligned} \dot{\mathbf{x}} &= \mathbf{A}\mathbf{x} + \mathbf{B}f + \mathbf{E}\ddot{x}_{\mathrm{g}} \\ \mathbf{y} &= \mathbf{C}_{\mathrm{y}}\mathbf{x} + \mathbf{D}_{\mathrm{y}}f + \mathbf{F}_{\mathrm{y}}\ddot{x}_{\mathrm{g}} + \mathbf{v} \\ \mathbf{z} &= \mathbf{C}_{\mathrm{z}}\mathbf{x} + \mathbf{D}_{\mathrm{z}}f \end{aligned} \tag{2}$$

where **x** is the state of the structure in terms of the bending and axial deformations from the center core and perimeter columns; **y** presents the measured structural responses including the relative displacements, the relative velocities, and the absolute floor accelerations; **v** is the measurement noise; **z** corresponds to the regulated structural responses.

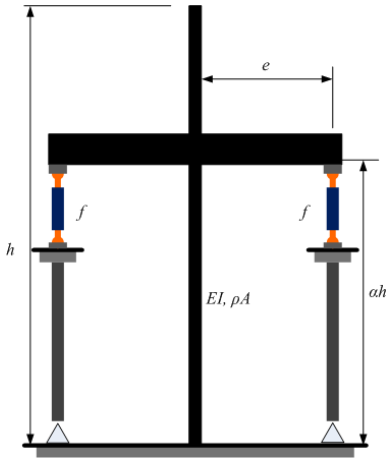

Figure 1. Mechanism of outrigger systems

3. REAL-TIME HYBRID SIMULATION

For real-time hybrid simulation (RTHS), the experimental setup in this study is configured by a MR damper connected to a servo-hydraulic actuator, as shown in Figure 2. The MR damper features a stroke of ± 25.4 mm and a 3 KN force capacity, and the actuators has a ± 152 mm stroke under a 3000 psi operating hydraulic pressure. To control the manifold and servo valve, the Schenck-Pegasus 5910 digital servo-hydraulic controller is used. For control implementation, a dSpace DS 1003 parallel processing DSP board based on a Texas Instrument TMS320C40 processor is adopted with a PC computer. With this system, a smart outrigger can be evaluated and experimentally verified for seismic protection of tall buildings.

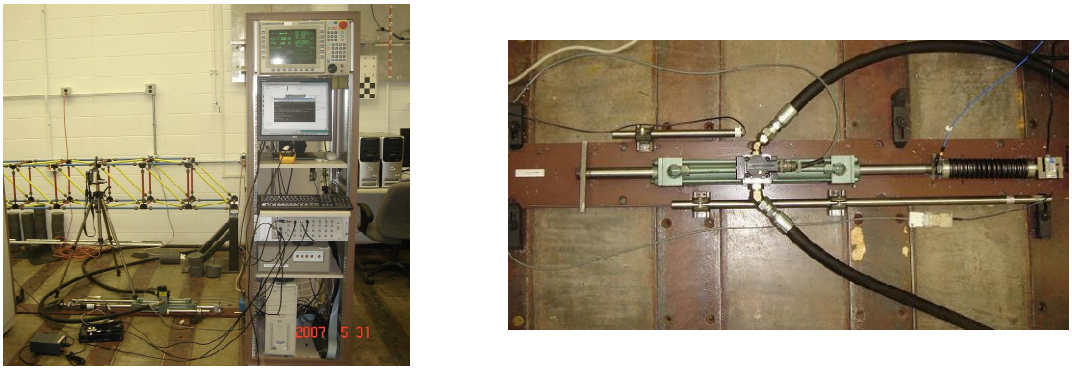

Figure 2. Experimental configuration for RTHS testing

To implement RTHS, the dSpace generates a command to the servo controller based on the predefined control law. The Schenck-Pegasus servo controller has a proportional-integral-differential control loop to operate the position control. On the actuator, a linear variable differential transducer (LVDT) and load cell acquire displacements and force for RTHS. These measurements are transmitted to the dSpace computer which calculated a required command to the servo valve for the next step. By closing this loop, RTHS is performed to assess smart outriggers.

The approach to facilitate RTHS is illustrated in Figure 3. This diagram displays a displacement-based RTHS of which displacements are tracked by imposing a feed-forward compensator. To develop the compensator, the RTHS system between the specimen (MR damper) and actuator is experimentally examined under BLWN excitation as the input (u) and subsequently characterized using a state-of-the-art identification tool, MFDID (Kim et al. 2005). The obtained transfer function represents the dynamics from the command (u) to the achieved displacement (x). Thus, the compensator is established by inverting the identified transfer function and then implemented in front of the displacement command (u). Due to the semi-active control strategies, different input voltages would alter currents to the MR damper, resulting in different transfer functions for the system. The compensator in RTHS consequently consists of a number of inverted transfer functions with respect to input voltage levels involved in the semi-active control strategies. In this study, only the 0 and 5 (maximum) volts are considered, and the compensator has two inverted transfer functions that are switched back and forth with a bumpless transition in the semi-active approaches.

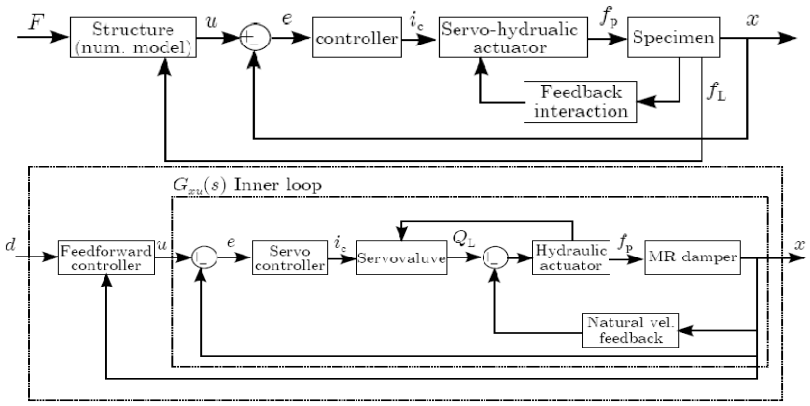

Figure 3. Control flow of RTHS testing

4. SEMI-ACTIVE CONTROL DESIGNS

To facilitate semi-active control using MR dampers, a control method that derives required force from adaptive input currents must be developed. Dyke et al. (1996a) proposed a LQG/clipped-optimal control method which had been verified through the experimental implementation with MR dampers. This study applies this control method for the smart outrigger system. In this control method, the outrigger system employs the H_2/LQG control algorithm to calculate the optimal control force and then switch on/off voltages for changing the input currents to the MR dampers. By reconsidering Eq. (2), the objective function of the H_2/LQG control can be written by

$$J = \lim_{\tau \to \infty} \frac{1}{\tau} E\left[\int_0^\tau \left(\mathbf{z}^T \mathbf{Q} \mathbf{z} + r f^2 \right) dt \right] \tag{3}$$

where $\mathbf{Q}$ and r are the weighting parameters. By minimizing Eq. (3), the control force is a function of the structural state. As different semi-active control strategies may be developed, the matrix $\mathbf{C_z}$ and $\mathbf{D_z}$ should be formed accordingly. In the H_2/LQG control, the Kalman filter estimates (Nagarajaiah and Narasimhan 2006) the state based on the measured responses such that

$$\begin{aligned} \dot{\hat{\mathbf{x}}} &= \mathbf{A}\hat{\mathbf{x}} + \mathbf{B} f_{\mathrm{m}} + \mathbf{L}\left(\mathbf{y} - \mathbf{C}_{\mathrm{y}} \hat{\mathbf{x}} - \mathbf{D}_{\mathrm{y}} f \right) \\ f_{\mathrm{d}} &= -\mathbf{K}_{\mathrm{c}} \hat{\mathbf{x}} \end{aligned} \tag{4}$$

where $\mathbf{L}$ is the Kalman gain; f_{d} denotes the desired force; $\mathbf{K}_{\mathrm{c}}$ is the optimal control gain; $\hat{\mathbf{x}}$ is the estimated state by the Kalman filter. To achieve the force calculated in Eq. (4), the clipped-optimal control approximates the command voltage by

$$v_{\mathrm{i}} = V_{\max} H\left\{ (f_{\mathrm{d}} - f) f \right\} \tag{5}$$

where $H\{\bullet\}$ is the Heaviside function; v_{i} is the input voltage to a MR damper; $V_{\max}$ is the maximum input voltage.

5. ST. FRANCIS SHANGRI-LA PLACE

The St. Francis Shangri-La Place in Philippines (Willford et al.2008) employs a damped outrigger system and provides the inspiration of this study. This structural system is used to assess the efficacy of the smart outrigger system. The St. Francis Shangri-La Place is a sixty-story building with a height of 210 m (Infanti et al. 2008). This building has 12 perimeter columns which are 20 m from the building centerline. The concrete core is assumed to be 12 m x 12 m with a 0.5 m thickness, and the cross section of the perimeter columns are 2 m x 2 m. The total mass of this building reaches 30,000 tons. The outrigger system implemented in this building consists of sixteen viscous dampers, eight of which control the response in each of the two orthogonal directions. Note that this study only considers unidirectional excitations.

As the assumption made previously, this high-rise building itself is modeled as a cantilever beam. The finite element model is comprised of 60 beam elements with 120 DOFs, including 60 translational and 60 rotational DOFs. The perimeter columns are modeled by a single DOF system of which the mass term is composed of the partial weight of the building. The modal damping is assumed to be 2 % for each mode. The natural frequencies of the first five modes are 0.18, 1.15, 3.14, 6.00, and 9.61 Hz, respectively. As a convectional outrigger wall is considered at different heights, the dynamic characteristics vary in accordance with the resulting vertical stiffness of the perimeter columns. Figure 4 illustrates the high-rise building with or without an outrigger wall at different levels. In the context of stiffness, the building with a mid-high outrigger wall produces a largest natural frequency at the first mode. By investigating the 1st mode shapes, the outrigger wall at 0.8 of the height can provide smaller top displacements, while the outrigger wall at the top would efficiently reduce the rotations. Note that each mode shape shown in Figure 2 has a vector norm equal to one.

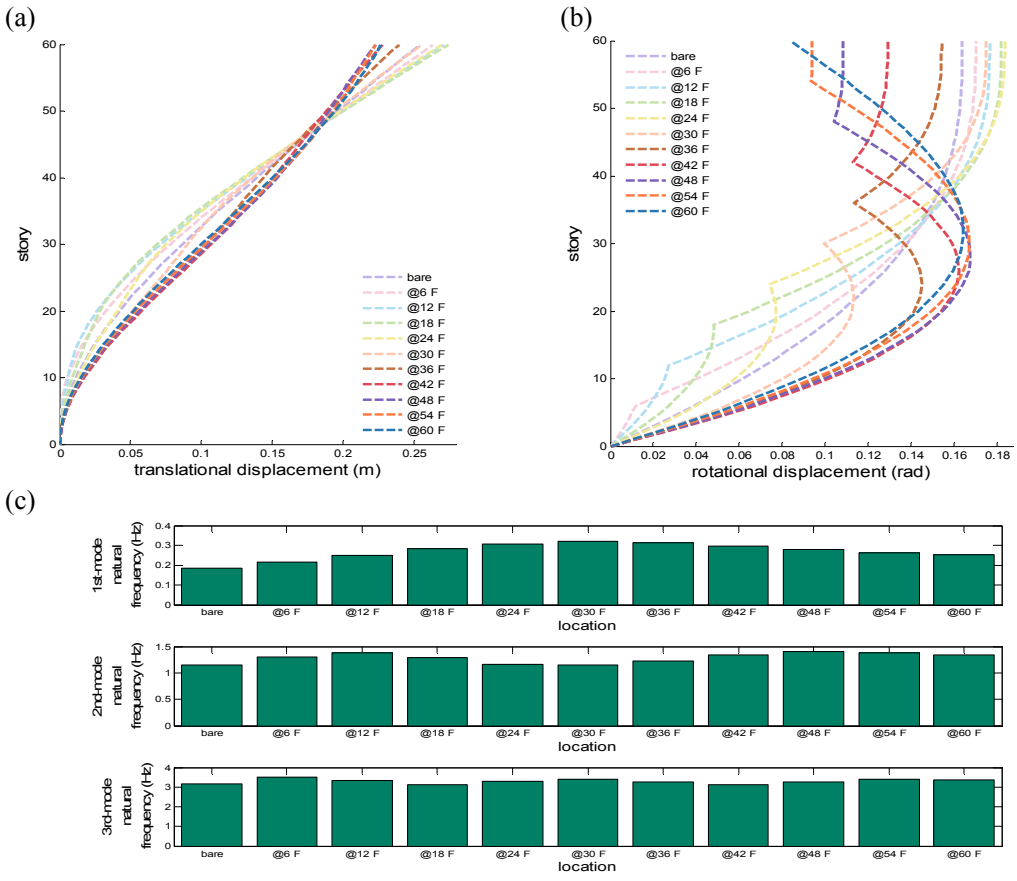

Figure 4. Modal analysis for (a) translational and (b) rotational 1st-mode shapes and (c) natural frequencies of first three modes

6. NUMERICAL AND EXPERIMENTAL RESULTS

This study numerically and experimentally verifies two smart outriggers against seismic loadings. The first case is to synthesize RTHS for a smart outrigger of which the building model is considered without the dynamics of the perimeter columns. The second case simulates the other smart outrigger in a building model that takes account for the vertical dynamics of the perimeter columns. In both cases, the location and MR damper size of the smart outrigger are determined by a proposed assessment method. Using the designed smart outriggers, the control performance is evaluated in comparison to other structural systems such as the uncontrolled building, building with an outrigger wall, and/or viscously damped outrigger.

The design of the location and damper size utilizes stochastic analysis to design the smart outriggers. Given an excitation spectrum, the root-mean-square (RMS) responses of structures can be calculated and analyzed. To examine a wide variety of damping coefficient and damper locations, structural responses are then computed by this stochastic approach. Therefore, the excitation spectrum adopts the Kanai-Tajimi spectrum with frequency $\omega_g = 12.6$ rad/sec and damping $\zeta_g = 0.3$ (Ramallo et al. 2002). The locations are discretized by 0.1 of the building height from the middle height to the top, and the damping coefficients per damper are increased by 5 MN-sec/m in a range of 5-800 MN-sec/m. For example, Figure 5 illustrates the design results for the smart outrigger of which the building model considers the dynamics of the perimeter columns. The performance index is normalized from the summation of weighted RMS responses that include the floor displacements, accelerations, base shears, and overturning moments. By investigating the concave of the performance surface, the best design for the smart outrigger is the one which has 80-90 MN-sec/m at the 54th floor as the building model considers the perimeter columns. Similarly, as the building excludes the perimeter columns, a 40 MN-sec/m damping coefficient and the 42th floor are obtained through the same method. As a result, the total number of MR dampers is 8 in each case as referred to the configuration in Willford et al. (2008). In the semi-active control approaches, the damping coefficients of MR dampers are approximately equivalent to the designed numbers.

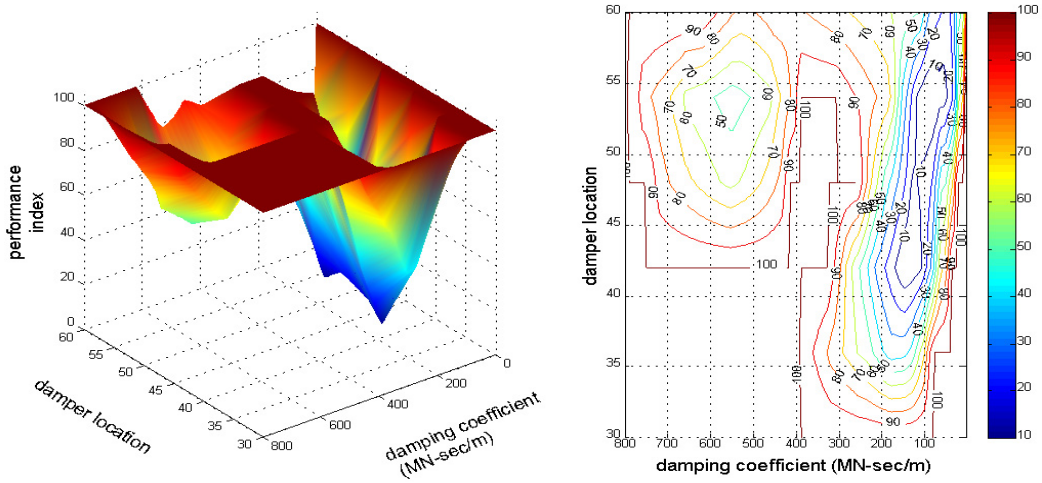

Figure 5. Design of damper sizes and locations for smart outriggers

6.1 Experimental Results

First, the smart outrigger using RTHS is introduced. As mentioned earlier, this test is conducted on a 3-KN MR damper. Assume that the outrigger wall moves rigidly across the entire wall and the perimeters do not contribute the dynamics of the structural system. To understand the behaviour of the smart outrigger, the MR damper is experimentally characterized based on a Bouc-Wen model, proposed by Spencer et al. (1997). Moreover, the feed-forward compensator is also inverted from the

command-to-displacement transfer functions with respect to 0 and 5 volts. These inverted transfer functions are formed as four-zero and zero-pole models. By considering a one-pole system, a transition from one input voltage to the other is generated for the phase change. Amplifying factors for force, displacement, velocity of the MR damper are also applied in order to match the designed damping coefficient (40 MN-sec/m). With this setup, the smart outrigger can be experimentally explored and verified.

The design of the semi-active controller is aimed at the minimization of the rotational displacements. To realize the feedback control, the floor accelerations at the 10^{th}, 20^{th}, 30^{th}, 40^{th}, 50^{th}, and 60^{th} floors are selected for the Kalman filter. The El Centro earthquake in Imperial Valley in 1940 is chosen for evaluating the smart outrigger. The peak ground acceleration (PGA) of this record is adjusted to be 0.3- and 0.5- g. The smart outrigger is performed in RTHS under a 2000 Hz sampling rate.

Figure 6 exhibits the smart outrigger results from the case of the El Centro earthquake. In Figure 6-a, the force difference between the RTHS and simulation is acceptable, but the slight difference implies the imperfection of the MR damper model that may overestimate the performance in simulation. According to Figure 6-b, the force-velocity relationship in the MR damper model has errors as compared to the one from RTHS. As a result, Figure 6-c shows better performance from the simulation than RTHS, indicating that an experimental approach for validation of a nonlinear, rate-dependent device is of need prior to implement same devices in the real-world structure. Furthermore, the semi-active control strategy provides high capability of mitigating displacements against earthquakes, while the MR damper delivers superior performance based on the designed damping coefficient. With the PGA level increase, the reductions on top displacements are more significant.

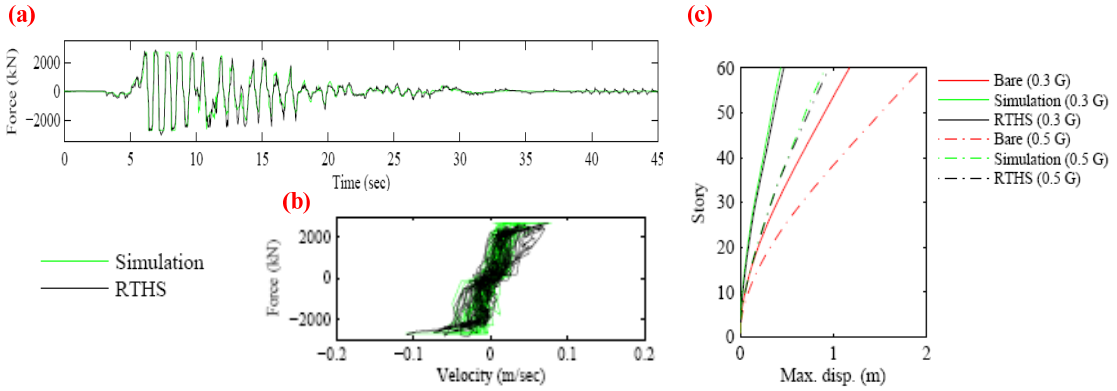

Figure 6. Smart outrigger results from RTHS

6.2 Numerical Results

The smart outrigger is presented as this control approach is applied to the building while considering the dynamics of the perimeter columns. In this portion, the smart outrigger employs a model for a prototype MR damper (Spencer et al. 1997). Likewise, the associated parameters of this model in terms of force, displacement, and velocity are appropriately adjusted. The maximum voltage used in the clipped-optimal control is set to be 5.0V, and the equivalent damping coefficient in the smart outrigger is approximately equal to the designed value (80 MN-sec/m per damper).

To evaluate the smart outrigger, the assessment is primarily aimed at the reductions on the relative displacements and overturning moments. In addition to the semi-active control strategies, the performance of the high-rise building with/without outrigger walls is discussed. A passively damped outrigger with 80 MN-sec/m viscous dampers is also considered. The maximum force of the viscous

dampers is limited to 6000 KN, and the yielding point of the force-velocity relationship of the MR dampers is designed approximately at a 5000-KN level.

In the context of ground excitations, two earthquake records are considered: 1) the north-south component of the El Centro earthquake in Imperial Valley, CA in 1940 and 2) the north-south component of the Kobe earthquake in Hyogo-ken Nanbu in 1995. The peak ground accelerations (PGA) of these records are normalized to four levels: 0.3 g, 0.5 g, 0.7 g, and 1.0 g.

Figure 7 shows the maximum and RMS displacement responses of the uncontrolled building and building with an outrigger wall. These responses are normalized to those from the building with a viscously damped outrigger. The translational displacements of the building with an outrigger wall vary with the seismic events. In the case of the Kobe earthquake, the responses of this structural system are significantly increased as compared to the uncontrolled building, indicating the necessity of additional damping devices for resisting seismic loadings.

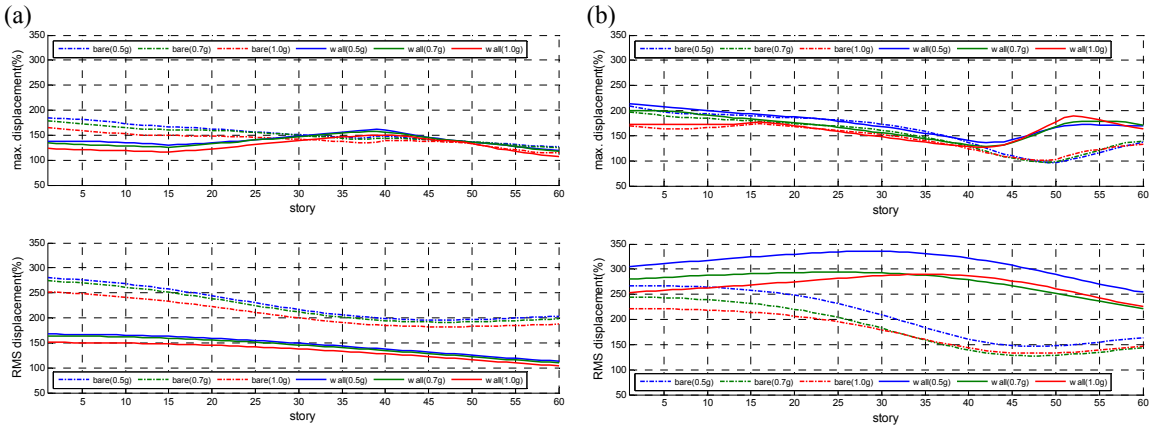

Figure 7. Comparison of control performance between the uncontrolled building and building with an outrigger wall under (a) El Centro earthquake and (b) Kobe earthquake

For the semi-active approach, the smart outrigger performs RMS displacements superiorly to the viscously damped outrigger, as shown in Figure 8. The responses in this figure are normalized to those from the viscously damped outrigger. The averaged reductions on RMS displacements are about 20% and 16% in both earthquake cases, respectively. As for the maximum displacements, the smart outrigger still produces better performance than the outrigger with viscous dampers in the El Centro earthquake case.

Figure 9 demonstrates the acceleration responses of the smart outrigger which are normalized by the responses from the viscously damped outrigger. Using the control objective of minimizing the floor accelerations, the smart outrigger produces smaller accelerations than the viscously damped outrigger. With the PGA increase, the RMS accelerations from the smart outrigger are better mitigated. Moreover, the normalized base shears and overturning moments to the viscously damped outrigger are shown in Figure 10. Despite some maximum floor accelerations exceeding 100%, most smart outrigger cases still generate lower maximum base shears and overturning moments. As a result, the smart outrigger can effectively decrease the maximum and RMS overturning moments up to 30% and 25% under the 1.0-g Kobe earthquake, as compared to the outrigger with viscous dampers. In sum, minimizing the translational floor accelerations from first thirty modes in the LQG/clipped-optimal control design performs a smart outrigger system better for this tall building against earthquakes.

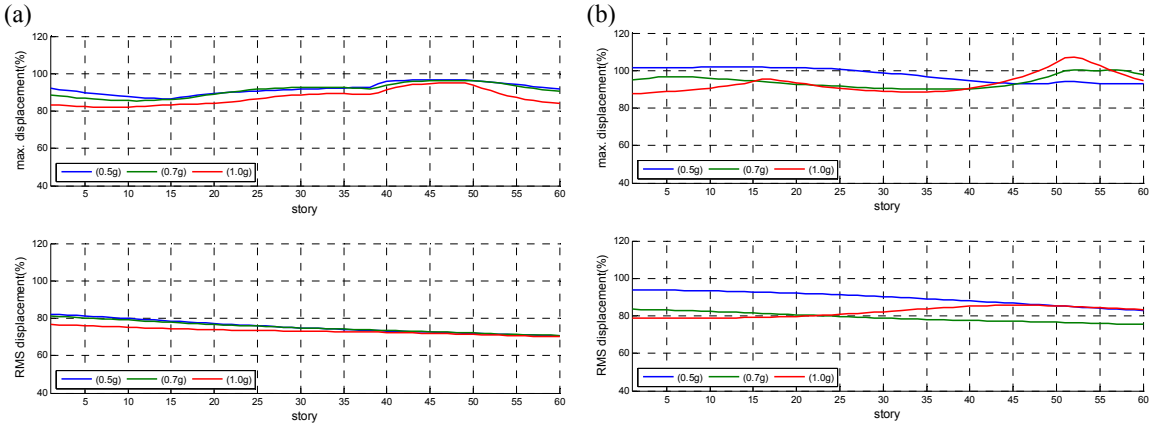

Figure 8. Displacements of the smart outrigger under (a) El Centro earthquake and (b) Kobe earthquake

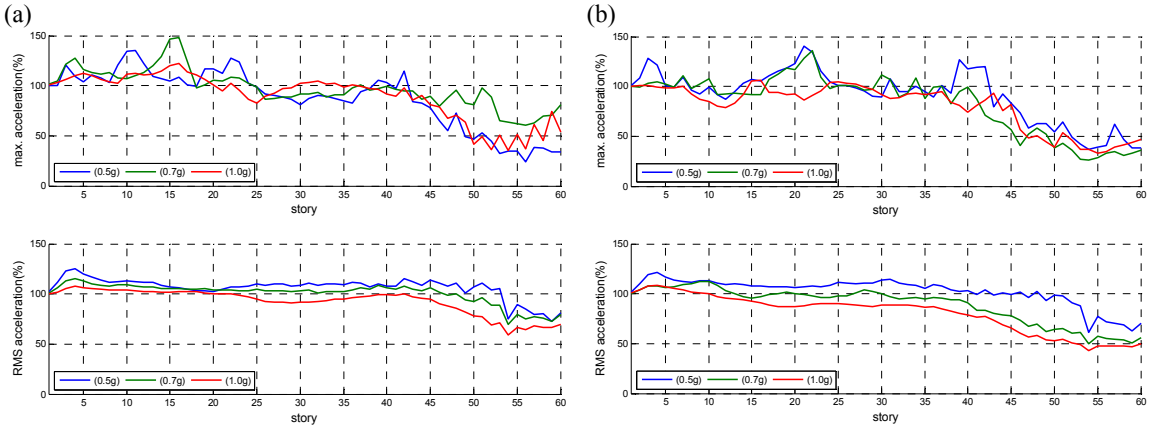

Figure 9. Floor accelerations of the smart outrigger under (a) El Centro earthquake and (b) Kobe earthquake

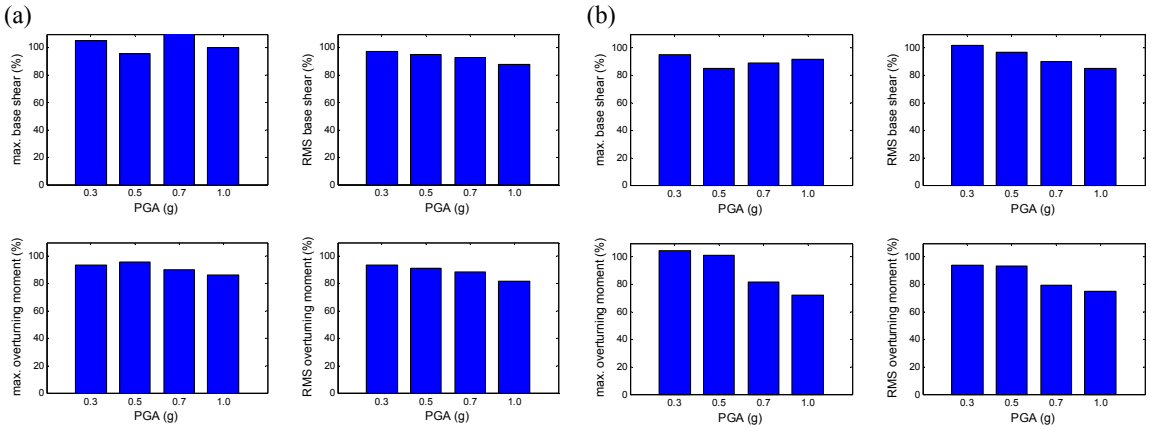

Figure 10. Base shears and overturning moments of the smart outrigger under (a) El Centro earthquake and (b) Kobe earthquake

7. CONCLUSIONS

This study developed and evaluated a smart outrigger system using MR dampers for a high-rise building. A building model was developed to portray the St. Francis Shangri-La Place in Philippines, and the smart outrigger system with a feasible configuration was determined. In the context of the

damper design, this study developed a method that evaluated the outrigger location and damper size through the stochastic analysis. By applying the proposed criteria, an optimal design was determined. To achieve high efficiency in the smart outrigger with MR dampers, the LQG/clipped-optimal control method was employed to design the semi-active control. Furthermore, this study also applied real-time hybrid simulation to test the smart outrigger. According to the results, a slight difference was found in results between the RTHS and simulation, indicating that the RTHS test can not only ensure the designed performance but also account for the modelling errors of the MR damper. In addition to the RTHS test, the numerical analysis was also conducted for the building with the perimeter columns considered. The numerical results showed that the semi-active controller provided high control performance against two historical earthquake loadings. The smart outrigger with the semi-active control strategies effectively generated sufficient dissipating energy through the outrigger arms as well as significantly created the high capability of mitigating the building displacements and overturning moments.

AKCNOWLEDGEMENT

The authors greatly acknowledged the partial support from the Chinese Scholarship Council. The authors would also like to acknowledge National Science Foundation's support under grants CMMI-0928886, Dr. S.C. Liu, Program Manager and the funding from National Science Council in Taiwan under Grant No. NSC-095-SAF-I-564-036-TMS.

REFERENCES

Dyke, S. J., Spencer, B. F., Jr., Sain, M. K., and Carlson, J. D. (1996). Modeling and control of magnetorheological dampers for seismic response reduction. Smart Materials and Structures, **5**, 565-575.

Infanti, S. and Robinson, J., and Smith, R. (2008). Viscous dampers for high-rise buildings. The 15th World Conference on Earthquake Engineering, Beijing, China.

Jeremlah, C. (2006). Application of damping in high-rise buildings. Massachusetts Institute of Technology, http://hdl.handle.net/1721.1/34589

Kareem, A., Kijewski, T., and Tamura Y. (1999). Mitigation of motion of tall buildings with recent applications. Wind and Structures, **2:3**, 201-251.

Ramallo, J. C., Johnson, A. M., and Spencer, B. F., Jr. (2002). "Smart" base isolation systems. Journal of Engineering Mechanics, **128:10**, 1088-1100.

Smith, B. S. and Salim, I. (1981). Parameter study of outrigger-braced tall building structures. Journal of Structural Division, **6**, 2001-2014.

Smith, R. J. and Willford, M. R. (2007). The damped outrigger concept for tall buildings. The Structural Design of Tall and Special Buildings, **16**, 501-517.

Spencer, B. F., Jr., Dyke, S. J., Sain, M. K., and Carlson, J. D. (1997). Phenomenological model of a magnetorheological damper. Journal of Engineering Mechanics, **3**, 230-238.

Smith, R. and Willford, M. (2007). The damped outrigger concept for tall buildings. The Structural Design of Tall and Special Buildings **16:4**, 501-517

Willford, M., Smith, R., Scott, D., and Jackson, M. (2008). Viscous dampers come of age. Structure Magazine, **6**, 15-18.

Yang, J. N., Agrawal, A. K., Samali, B., and Wu, J. C. (2004). Benchmark problem for response control of wind-excited tall buildings. Journal of Engineering Mechanics, **130:4**, 437-446.